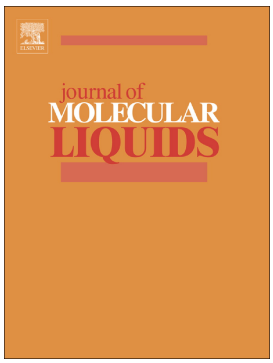

Phospholipid multilamellar vesicles entrapping phenothiazine photosensitizers. Preparation, characterization and evaluation of their photodynamic properties

Jimena Vara, Julieta M. Sanchez, María A. Perillo, Cristina S. Ortiz

PII: S0167-7322(18)33465-2
DOI: doi:10.1016/j.molliq.2018.10.009
Reference: MOLLIQ 9754

To appear in: *Journal of Molecular Liquids*

Received date: 5 July 2018
Revised date: 26 September 2018
Accepted date: 2 October 2018

Please cite this article as: Jimena Vara, Julieta M. Sanchez, María A. Perillo, Cristina S. Ortiz , Phospholipid multilamellar vesicles entrapping phenothiazine photosensitizers. Preparation, characterization and evaluation of their photodynamic properties. Molliq (2018), doi:10.1016/j.molliq.2018.10.009

Phospholipid multilamellar vesicles entrapping phenothiazine photosensitizers. Preparation, characterization and evaluation of their photodynamic properties.

Jimena Vara[a,b], Julieta M. Sanchez[c,d], María A. Perillo[c,d**] and Cristina S. Ortiz[b*]

[a] CONICET, UNITEFA, Córdoba, Argentina.

[b] Universidad Nacional de Córdoba, Facultad de Ciencias Químicas, Departamento de Ciencias Farmacéuticas, Córdoba, Argentina.

[c] CONICET, IIBYT, Córdoba, Argentina.

[d] Universidad Nacional de Córdoba, Facultad de Ciencias Exactas, Físicas y Naturales, Departamento de Química, Cátedra de Química Biológica, Córdoba, Argentina.

[*]Corresponding Author: e-mail address: crisar@fcq.unc.edu.ar

[**] Co-Corresponding Author: e-mail address: mperillo@unc.edu.ar

HIGHLIGHTS

- Azure B and its monobrominated derivative were encapsulated in multilamellar liposomes
- Liposome encapsulation decreased the aggregation of phenothiazine dyes
- Encapsulated photosensitizers exhibited higher singlet oxygen quantum yield

ABSTRACT

The aim of the present paper was to optimize the properties of phenothiazine photosensitizers (PSs), Azure B and its monobrominated derivative. They were entrapped in multilamellar liposomes of egg phosphatidylcholine (EPC) and dipalmitoylphosphatidylcholine (dpPC). The higher partition coefficient of both PSs in the EPC/water system compared with that of both PSs in the dpPC/water system allowed the selection of EPC to be used for the development of third generation photosensitizers. The optimal phospholipid/phenothiazine ratio and the location of these dyes in the lipid bilayer systems were established. These dyes were found to be located within the polar head group region of the lipid bilayer, which would enhance the effectiveness of the irradiation procedure. In addition, the encapsulation of both photosensitizers in liposomes led to a decrease in the aggregation of these compounds, and consequently to an increase in their singlet oxygen quantum yield (ϕ_Δ). The encapsulation of the PSs in lipid vesicles significantly increased their photochemical reactivity, doubling the ϕ_Δ value of AzBBr and increasing that of AzB by 60%. The results obtained demonstrate that the vehiculization of these PSs in liposomes allowed the development of third generation photosensitizers with better photochemical properties to be used in potential therapeutic applications.

KEYWORDS

Phenothiazine dyes, photochemical properties, EPC, dpPC, encapsulation efficiency of MLVs, membrane partitioning and location.

1 INTRODUCTION

The exposure of Photosensitizers (PSs) to a specific light wavelength induces the production of harmful radicals such as reactive species of oxygen (mainly singlet oxygen, $^1O_2$) and nitrogen, which are capable of killing cells.[1,2] PSs are used in Photodynamic Therapy (PDT) as a valuable alternative for the diagnosis and treatment of various types of cancers. It is known as Antimicrobial Photodynamic Therapy (APDT) when it is applied to the treatment of diseases caused by a broad range of species of microorganisms, regardless of drug resistance.[3] Both therapies provide a safe and effective way to selectively eradicate target cells while avoiding systemic toxicity and side effects on healthy tissues.[4] For this reason, PDT and APDT are widely evaluated to address two global issues of health, the treatment of cancer and antibiotic resistance, which are a priority for the World Health Organization (WHO). Consequently, the development of new PSs and different alternatives to improve the effectiveness of these therapies has become an important field of scientific research.

The clinical use of first and second generation PSs has been questioned because of their low selectivity, hydrophobicity, and important biodegradation, among other features. In order to overcome these difficulties, different vehiculization strategies are used, which allow obtaining biodegradable systems, known as third generation PSs.[5,6] There are different drug delivery approaches that can be used for the diagnosis and treatment of numerous diseases Examples of the main nanocarriers used in the field of medicine include micelles, liposomes, dendrimers, carbon nanotubes, nanoshells, and gold, silver and copper nanoparticles.[7–15]

Liposomes are currently one of the most commonly used drug nanocarrier systems in clinical applications and are particularly employed in the treatment of various oncological diseases.[16] These strategies are widely investigated for their use in PDT and APDT because they are versatile systems capable of encapsulating hydrophilic, hydrophobic, and amphiphilic molecules. Liposomes exhibit high biocompatibility and increase the amount of PS available at the site of action, preventing its degradation and aggregation in the biological environment, as well as reducing unspecific damage.[17–19] In addition, numerous studies proved that the use of liposomes for the development of third generation PSs has greater benefits than other delivery systems, such as micelles and polymeric or metallic nanoparticles.[20,21]

Encouraging results were obtained by using conventional liposomes as nanocarriers for PDT and APDT. Visudyne®, a liposomal formulation of verteporfin, is one of the first third generation PSs approved by FDA in 2000 for the treatment of age-related macular degeneration. Foslip® is another recently developed third generation PS based on a liposomal formulation, which is in preclinical phases. [13,14] Several experimental results showed that liposomal formulations exhibit greater photodynamic efficiency and cause less damage to healthy tissue. Also, these formulations are less toxic in the absence of light compared with the free PS. [15, 16] In conclusion, the encapsulation of different PSs is a successful strategy to increase the photoinactivation of bacteria and numerous tumor cells, as well as to reduce toxicity and damage to healthy tissue in darkness.

The purpose of this study was to encapsulate Azure B (AzB) and its novel monobrominated derivative (AzBBr) in multilamellar liposomes (MLVs). These vesicular systems were selected to carry out biophysical studies and, as a first step, to develop third generation PSs, since they can encapsulate a high concentration of lipophilic and amphiphilic drugs, are easy to prepare and are mechanically stable during storage.[26,27] In this approach, we evaluated the effect of MLVs on the aggregation of PSs and consequently on the production of singlet oxygen. Previous studies have demonstrated that phenothiazine dyes form higher order aggregates in aqueous media, which decreases their photodynamic efficacy.[28,29] The encapsulation of AzB and AzBBr in liposomes would be an interesting strategy to prevent their aggregation in biological media and improve their properties as PSs.

2 MATERIALS AND METHODS

2.1 Chemicals

AzB was purchased from Sigma Aldrich Co. (St. Louis, MO) and used without additional purification, while AzBBr was synthesized by the method previously described.[30] **Figure S1** (see Supporting Information) shows the chemical structure of both compounds, which were used at higher purity levels (greater than 95%).

The lipids, egg-phosphatidylcholine (EPC) and dipalmitoylphosphatidylcholine (dpPC), employed for the preparation of liposomes were purchased from Avanti Polar Lipids (Alabaster, Alabama) and used without further purification. The fluorescent probes, diphenylhexatriene (DPH), trimethyl-ammonium-diphenylhexatriene (TMA-DPH), and 9,10-Anthracenediyl-bis (methylene) dimalonic acid (ABDA), were obtained from Sigma Chem. Co (St. Louis, MO). Phosphate-buffered saline (PBS, 150 mM pH 7.4) solution was prepared using ultrapure water from a Milli-Q® purification system. All reagents and solvents used were of analytical grade.

2.2 Instrumentation

Absorption spectra were carried out at room temperature with a Cary 60 UV-Vis (Agilent Technologies) spectrophotometer between 200 and 800 nm using a 1 cm length quartz cell.

Fluorescence spectra were recorded on a Fluoromax Spex-3 Jobin Yvon (Horiba, NJ, USA) spectrofluorometer equipped with a thermostatized cell, a Xenon arc lamp, and a diode array detector, where light intensity was registered by a photon counter system. The excitation and emission slits were 0.5 nm wide. Excitation wavelength (λ_{ex}) and emission wavelength (λ_{em}) were determined for each experiment.

Liposome size and polydispersity index (PI) were determined by dynamic light scattering (DLS) at 25 °C using a Beckman Coulter DelsaTM Nano C Particle Analyser with a He-Ne laser (633 nm), a scattering angle of 165°, a viscosity of 0.8878 Pa, and a refractive index of 1.3328. The samples were appropriately diluted with water before their analysis. A minimum of three measurements were taken and averaged for each determination.

2.3 Preparation of liposomes

MLVs were prepared by the film-hydration method.[31] Different concentrations of lipids (EPC or dpPC) and PSs (AzB or AzBBr) were dissolved in chloroform/methanol (2:1 v/v). The solvents were then evaporated under a stream of nitrogen with constant rotation of a test tube so as to deposit a uniform film over the bottom third of the tube. Traces of solvents were removed under vacuum. The lipid film was rehydrated with PBS by vortexing at a temperature above the gel to liquid-crystalline phase transition of the lipids to obtain MLVs.

2.4 Effect of liposome encapsulation on the aggregation properties of photosensitizers

In order to select the optimal MLVs for the entrapment of the phototherapeutic agents AzB and AzBBr, the effect of the encapsulation of these compounds in vesicles of EPC and dpPC on the aggregation of PSs was evaluated. MLVs were prepared as mentioned in the previous section using 1 mg/mL of lipids (EPC or dpPC) and different concentrations of PSs (5-45 μM). The resulting samples were analyzed by UV-Vis spectrophotometry. The intensity absorption ratio of the two bands corresponding to the dimer ($\lambda_{max-abs}^{AzB}$: 646 nm; $\lambda_{max-abs}^{AzBBr}$: 650 nm) and high aggregates ($\lambda_{max-abs}^{AzB}$: 600 nm; $\lambda_{max-abs}^{AzBBr}$: 601 nm) was calculated at the maximum absorption wavelength ($\lambda_{max\text{-}abs}$).[28] These values were compared with those obtained for AzB and AzBBr in PBS without lipids. The higher values of this ratio indicated higher disaggregation of the dyes.[32]

2.5 Optimization of liposomal formulation

To select the optimal EPC/PS ratio that allows the highest incorporation of the dyes into the liposomes, the encapsulation efficiency (EE) of different liposomal preparations was evaluated by UV-Vis spectrophotometry. Prior to testing EE, it was necessary to select a detergent (DT) to destabilize MLVs and subsequently quantify the PSs.

2.5.1 Selection of detergent for liposome lysis

The treatment of biomembranes with an excess of DTs produces mixed (DT-phospholipid) micelles. This new environment may affect the absorption, excitation, and emission properties of drugs. Therefore, the absorption and fluorescence intensities (FI; λ_{ex}: 646 nm and 650 nm for AzB and AzBBr,

respectively; λ_{em} range: 660 - 850 nm) of aqueous solutions of PSs were evaluated in the presence and in the absence of different DTs. The effect of anionic (sodium dodecyl sulfate, SDS), cationic (cetyl-trimethyl-ammoniumbromide, CTAB), and non-ionic (Triton X-100) DTs was tested. Solutions of AzB and AzBBr in PBS at different concentrations (1.5 - 20 μM) were analyzed. DTs were applied at either 0 or 35 mM. The higher concentration was well above the critical micelle concentration (cmc) of each tested DT.[33] It is important to note that the treatment with SDS could not be processed due to the formation of abundant precipitate.

Absorption spectra were determined between 200 nm and 800 nm at room temperature using a quartz cell with an optical path length of 1 cm. Fluorescence spectra were recorded between 660 nm and 850 nm. The selected λ_{ex} were the $\lambda_{max\text{-}abs}$ corresponding to the dimeric species of PSs (646 nm and 650 nm for AzB and AzBBr, respectively).[28]

2.5.2 Determination of encapsulation efficiency

EE was determined as a function of lipid (1 - 30 mg/mL) and PS (36 - 360 μM) concentrations by UV-Vis spectrophotometry. MLVs of EPC or dpPC were prepared in a final volume of 2 mL. Half of the sample volume was used to determine 100% of PS (PS_{total}). The second half aliquot was centrifuged for 15 min at 10000 rpm. Subsequently, the supernatant was separated and the pellet obtained was resuspended in 1 mL of PBS. Finally, Triton X-100 (35 mM) was added to the non-centrifuged samples (PS_{total}), supernatants (PS_{free}), and resuspended pellets ($PS_{encapsulated}$). The samples were analyzed by UV-Vis spectrophotometry. The percentage of encapsulated PS was determined by **Equations 1** and **2**. The results obtained were the mean ± SD of both determinations.[34]

$$\boldsymbol{EE}\ (\%) = \frac{\boldsymbol{Abs_{PS\ encapsulated}}}{\boldsymbol{Abs_{PS\ total}}}\ \boldsymbol{x}\ \mathbf{100}\% \qquad \textbf{Equation 1}$$

$$\boldsymbol{EE}\ (\%) = \frac{\boldsymbol{Abs_{PS\ total} - Abs_{PS\ free}}}{\boldsymbol{Abs_{PS\ total}}}\ \boldsymbol{x}\ \mathbf{100}\% \qquad \textbf{Equation 2}$$

Note that the concentration of AzBBr charged in MLVs was calculated using a molar absorptivity coefficient value, ε= (18.4 ± 0. 6) x 10^3 $M^{-1}cm^{-1}$, previously defined in a Triton X-100/EPC mixture (27:1 molar ratio) in PBS (data not shown).

2.6 Interaction photosensitizer–multilamellar vesicles

2.6.1 Evaluation of membrane-water partition coefficient

Due to the amphiphilic characteristics of AzB and AzBBr, the membrane-water partition coefficients (K_p) of these PSs were evaluated.

The values of K_p were estimated according to the method described by Lissi et al.[35] The methodology used is based on the evaluation of a property that depends on the degree of partition of the dye. It is a simple method, suitable for the use of spectroscopic techniques and does not require the separation of membrane from aqueous solution phases. For the determination of K_p, it is assumed that the magnitude of the observed effect is determined only by the concentration of the solute in the membrane.[35]

These tests involved the spectrophotometric evaluation of the aggregation of PSs (effect that depends on the extent of partitioning into the lipid interface), as a function of the dye concentration (8 - 46 μM) at different membrane volumes (V_M: 0 - 1 μL of EPC) and at a constant volume of the aqueous phase (V_w: 1mL).[35] In the first instance, the slopes (S_1) corresponding to dimer/higher-order aggregate absorbance ratio (Abs^D/Abs^{HA}) as a function of the moles of PSs were determined for different EPC volumes (**Scheme 1**). The reciprocal of the slopes obtained ($1/S_1$) was plotted as a function of the V_M (**Scheme 2**). The values of K_p were determined from the slopes (S_2) and y-intercepts (Y_2) corresponding to the second graphic according to **Equation 3**.

$$Abs^D/Abs^{HA} \quad vs \quad PS\ moles \longrightarrow S_1 \qquad \textbf{Scheme 1}$$

$$1/S_1 \quad vs \quad V_M \longrightarrow S_2 \text{ and } Y_2 \qquad \textbf{Scheme 2}$$

$$K_p = \frac{S_2 \times V_w}{Y_2} \qquad \textbf{Equation 3}$$

It is important to note that MLVs were prepared as described in Section 2.3. All samples obtained were analyzed by UV-Vis spectrophotometry.

2.6.2 Localization of the photosensitizers in phospholipid bilayer

The fluorescence resonance energy transfer (FRET) between fluorescent probes and PSs was evaluated in the presence and in the absence of liposomes. The probes used were DPH, known to be located within the lipophilic region of the membrane (hydrocarbon chain of phospholipids), and TMA-

DPH, which stabilizes its cationic moiety at the polar head group of the phospholipids (surface of the lipid bilayer).[36] MLVs were prepared with 0.5 mg/mL of EPC and 80 μM of PSs by the methodology previously descripted. Then, stock solutions of DPH or TMA-DPH (1.15 - 15 μM) were added to the liposomal formulation 1 h before the analysis of the samples. Steady state fluorescence spectra were recorded from 380 nm to 750 nm, with the emission set at 356 nm.

In order to corroborate that FRET only occurs when the probes and PSs are bound to MLVs, solutions of AzB and AzBBr (80 μM) with different concentrations of DPH or TMA-DPH (1.15 - 15 μM) were evaluated in PBS without liposomes.

2.7 Singlet oxygen quantum yields

The $^1O_2$ production of the AzB and AzBBr encapsulated in MLVs of EPC was evaluated indirectly analyzing ABDA photooxidation by UV-Vis spectrophotometry at different irradiation times. [21,37] The results obtained were compared with those previously published for free PSs in aqueous solution by employing the same methodology.[29]

Liposomal samples were prepared using 15 mg/mL of EPC and 260 μM of the phototherapeutic agents AzB or AzBBr (see Section 2.3). The MLV suspensions were centrifuged for 15 min at 10000 rpm in order to separate free from encapsulated PS. The pellets obtained (MLV + PS encapsulated) were resuspended in ultrapure water. Before starting the photooxidation test, an aliquot of ABDA aqueous solution, enough to reach an absorbance of around 0.3 at 380 nm, was added to the liposomal samples.

The samples were irradiated for 360 s using a Parathom® LED lamp (5w - OSRAM) and analyzed at different times by UV-Vis spectrophotometry using a quartz cell with an optical path length of 1 cm. The irradiance intensity at a 5 cm distance was 8.4 mW/cm2. The absorbance values at 380 nm were plotted as a function of the irradiation time. The obtained slopes (k_{obs}) allowed the determination of the relative singlet oxygen quantum yields (ϕ_Δ) according to **Equation 4**, where Abs_0^{PS} is the absorbance of third generation PSs and Abs_0^{Ref} is the absorbance of references at the initial time of the assay. The values obtained for ϕ_Δ were determined using the free forms of AzB and AzBBr as references. All assays were performed in duplicate, demonstrating consistent results.

In order to corroborate that the oxidation of ABDA occurs only by the action of the $^1O_2$ generated by the excitation of PSs, samples equivalent to those irradiated were analyzed at different times and protected from light. Also, the behavior of ABDA against irradiation in the presence of MLVs without phenothiazine dyes was evaluated.

$$\Phi_{\Delta}^{PS} = \frac{\Phi_{\Delta}^{Ref} k_{obs}^{PS} Abs_0^{Ref}}{k_{obs}^{Ref} Abs_0^{PS}}$$ **Equation 4**

3 RESULTS AND DISCUSSION

3.1 Preparation of liposomes

Dynamic light scattering (DLS) assays confirmed the formation of vesicular systems. The values obtained for the particle size of EPC (0.95 μm) and dpPC **(**1.2 μm) were consistent with the presence of MLVs, considering mainly the method used for their preparation. It has been reported that MLVs have a size of between 0.5 -10 μm [38], while the film hydration method leads to the formation of heterogeneous multilamellar liposomes with an average diameter of 1-5 μm.[39] Moreover, the polydispersion index (PI = 0.3) determined for both samples showed their quite homogeneous particle size distribution. In conclusion, the methodology used allowed the obtainment of appropriate liposomal preparations for the development of novel third generation PSs.

3.2 Effect of liposome encapsulation on the aggregation properties of photosensitizers

The plots of absorbance ratio (dimer / higher order aggregate, Abs^{D}/Abs^{HA}) as a function of the PS concentration for AzB and AzBBr, both free and encapsulated in MLV of EPC and dpPC, are shown in **Figure 1**.

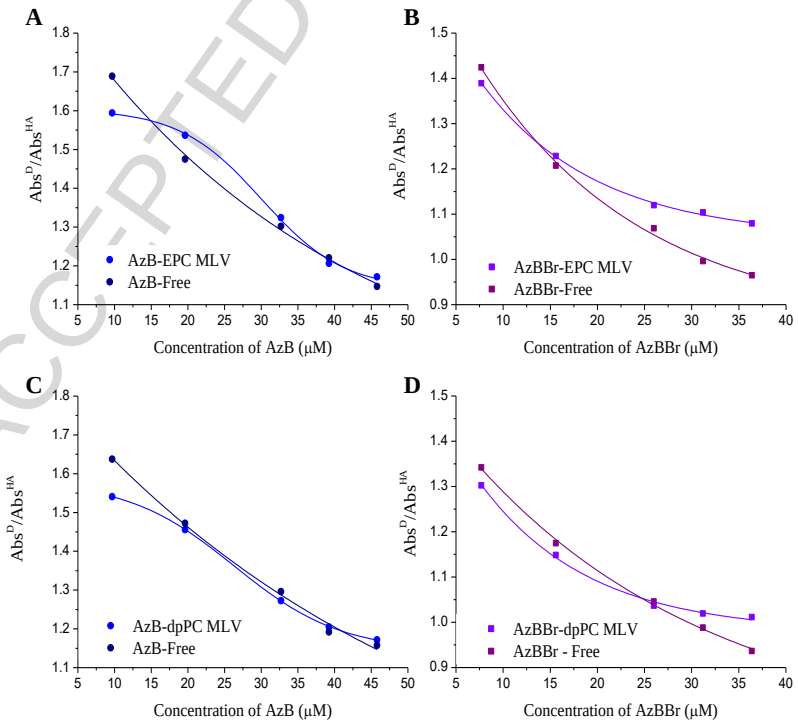

Figure 1: Evaluation of aggregation of AzB and AzBBr, free and encapsulated in MLVs of EPC (**A** and **B**) or dpPC (**C** and **D**).

The trends of the aggregation curves of AzB in aqueous solution and trapped in liposomes differed from one another (**Figures 1A** and **1C)**. While the free PS exhibited an exponential behavior, the entrapped dye showed a sigmoidal decay. However, there was no significant difference in the aggregation of AzB encapsulated in MLV of EPC or dpPC over the concentration range evaluated. The monobrominated derivative, in contrast, showed an exponential decay for both free and encapsulated PS (**Figures 1B** and **1D**), evidencing important differences at the highest dye concentrations tested. High values of Abs^{D}/Abs^{HA} indicated a predominance of the dimeric form over higher order aggregates, which means a decrease in the aggregation and stabilization of the active species of these compounds.[29,40] In summary, the aggregation of the encapsulated AzBBr decreased compared with that of the free PS at the higher concentrations tested. In addition, the EPC vesicles were more efficient than those of dpPC at preventing the aggregation of PSs. This behavior suggests that AzBBr has a greater tendency to partition into the EPC liposomes compared with those composed of dpPC due to the lower molecular packing of the former at the assayed temperature. Considering that the gel-to-liquid crystalline transition temperature is below 0°C and 41.5°C for EPC and DPPC, respectively, it can be predicted that the preference of PSs for partitioning in EPC over DPPC will remain in physiological conditions. The higher partitioning of PS also explains why EPC is more efficient at preventing the formation of higher order aggregates. For this reason, EPC-MLVs were selected to develop the third generation PSs.

3.3 Optimization of liposomal formulation

3.3.1 Selection of detergent for liposome lysis

The absorption spectra of the phototherapeutic agents AzB and AzBBr were determined in PBS in the absence and in the presence of CTAB and Triton X-100 (see Figure S2 in Supporting Information). While both detergents induced a decrease in the tendency of PSs to aggregate, mainly in the presence of Triton X-100, the formation of higher order aggregates was inhibited and the active species of both PSs were stabilized.

Figure 2 shows the results obtained from the fluorescence studies of the PS in the presence and in the absence of the different detergents, using as λ_{ex} the maximum absorption of the dimeric species of AzB and AzBBr. An increase in fluorescence intensities (FI) was observed with the increase in the

concentrations of both PSs in diluted solutions (≤ 10 μM). However, at higher concentrations, samples exhibited a decrease in FI. In addition, the normalized curves at the maximum emission wavelength ($\lambda_{max\text{-}em}$) showed that the increase in the PS concentration produced a bathochromic shift of the spectral curves (**Figure 2, inserts**). This behavior has been previously reported for phthalocyanine compounds and was attributed to a fluorescence reabsorption effect. [41] This behavior is independent of the formation of aggregates.

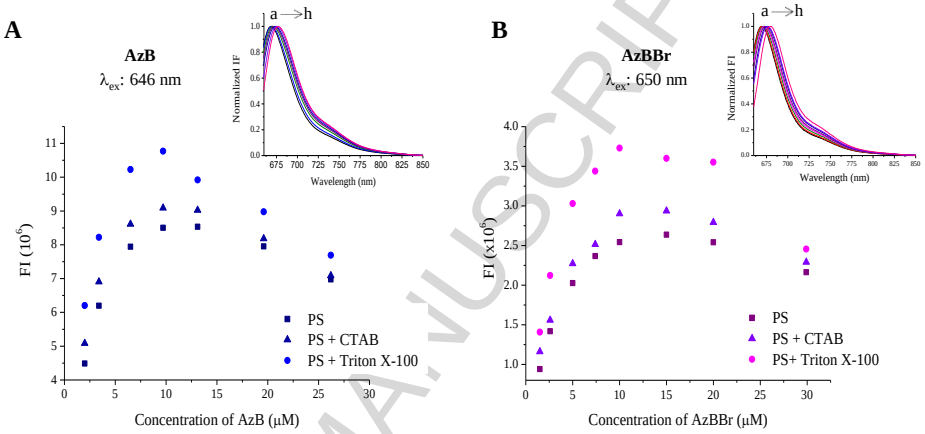

Figure 2: Fluorescence intensity (FI) vs. the concentration of AzB (**A**) and AzBBr (**B**) in PBS in the absence and in the presence of different DTs. **Insert**: Normalized fluorescence spectra at $\lambda_{max\text{-}em}$ at different concentrations of PSs. Arrows point to the direction observed with increasing concentration of PSs: (a) 1.5 μM; (h) 30 μM.

To determine the effect of DTs on the aggregation of AzB and AzBBr by fluorescence spectroscopy, the FI of the samples at the same concentration of the PSs were compared in the presence and in the absence of different DTs. Other researchers have shown that H-aggregates (which exhibit hypochromic changes) have no fluorescence and lead to efficient fluorescence quenching of other species in solution.[42–44] For this reason, an increase in FI during the test indicated an increase in the proportion of the dimeric species and consequently a decrease of the higher order aggregates. As shown in **Figure 2,** both evaluated DTs decreased the aggregation of AzB and its monobrominated derivative, which corroborates the results obtained by UV-Vis spectrophotometry. In addition to absorbance measurement, the FI data shows that Triton X-100 presented the greatest effect on the stabilization of the

dimeric species. A similar behavior of Triton X-100 was described by Camur et al. for phthalocyanines in aqueous solutions.[45]

To conclude, Triton X-100 inhibited the formation of higher order aggregates of phenothiazine dyes in aqueous medium, stabilizing the dimeric species of AzB and AzBBr. These results support the selection of this DT for the destabilization of MLVs in the subsequent quantification of the PSs under study.

3.3.2 Determination of encapsulation efficiency

In order to evaluate the effect of the EPC concentration on the EE of AzBBr, MLVs prepared from different lipid concentrations (1- 30 mg/mL) were analyzed keeping the PS concentration (36 μM) constant. As shown in **Figure 3A**, the incorporation of the monobrominated derivative into the vesicular system increased exponentially as a function of the EPC concentration. The maximum EE was 88% at phospholipid concentrations ≥ 15 mg/mL.

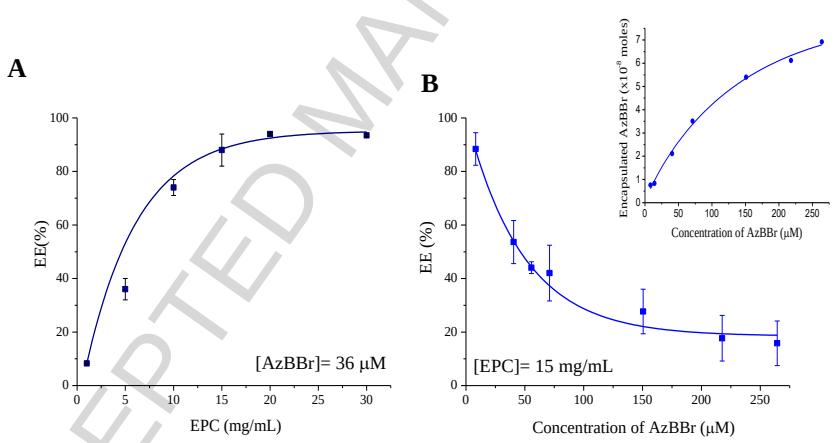

Figure 3: Encapsulation Efficiency (EE) of AzBBr in EPC MLVs as a function of lipid (**A**) and AzBBr (**B**) concentrations. **Insert**: Encapsulated mass of PS vs. the dye concentration used for the preparation of MLVs.

While EE decreased exponentially with increasing concentrations of AzBBr in the range of 36 to 260 μM (**Figure 3B**), the incorporation of this compound into the vesicular system increased considerably, achieving a maximum encapsulation of $7x10^{-8}$ moles (**Figure 3B, insert**).

Therefore, 15 mg/mL EPC and 260 μM AzBBr, which correspond to the maximum values in **Figures 3A** and **3B insert**, respectively, were selected as the optimal concentrations to develop the third

generation PS. Higher concentrations of lipid and dye in the preparation of MLVs would not significantly improve the EE of the system.

The optimal EPC/PS ratio established for the vehiculization of AzBBr was used to determine the EE of AzB. The obtained results indicated that MLVs trapped $8x10^{-8}$ moles of the commercial phenothiazine dye.

In summary, 15 mg/mL of EPC and 260 μM of the monobrominated phototherapeutic agent were selected as the optimal conditions to charge this PS and used to determine the amount of AzBBr and AzB trapped in the MLVs of EPC. These conditions allowed the encapsulation of $8x10^{-8}$ moles and $7x10^{-8}$ moles of AzB and AzBBr, respectively.

3.4 Interaction photosensitizer–multilamellar vesicles

3.4.1 Evaluation of membrane-water partition coefficient

Table S1 (see Supporting Information) shows the values obtained for the linear fitting of Abs^{D}/Abs^{HA} *vs PS moles* determined at different V_M (**Scheme 1**). This linear behavior allowed the determination of the membrane/water partition coefficients of AzB and AzBBr. For this, the reciprocal of $\mathbf{S_1}$ obtained for each PS was plotted as a function of V_M (**Scheme 2)** to determine the K_p of the phenothiazines evaluated using **Equation 3** (see **Figure S3**, Supporting Information).

The log K_p values obtained for AzB and AzBBr were 2.29 and 2.54, respectively. These results indicate that both phototherapeutic agents have a higher affinity for the lipid bilayer membrane than for the liposomal aqueous core. It is important to note that bromination increased the membrane partitioning of phenothiazine compounds. This result is consistent with the increased lipophilicity observed by Montes de Oca et al. for AzBBr compared with AzB in the determination of Log P_{HPLC}.[30]

3.4.2 Localization of photosensitizers in phospholipid bilayer

Förster energy transfer (FRET) is a probabilistic event based on the radiation-less transfer of excitation energy from a donor to an acceptor. FRET depends on the degree of spectral overlap between the donor and acceptor. Moreover, because the interaction between the donor and acceptor is a dipole-dipole interaction, FRET is a distance-and orientation-dependent interaction. The energy transfer occurs typically over a distance of 1-10 nm.[46]

The absorption band attributable to the phenothiazine compounds, AzB and AzBBr, presented a slight overlap with the emission bands of DPH and TMA-DPH (**Figure 4A**). These results suggest that the transfer of energy between the selected probes (DPH and TMA-DPH) (donors) and PSs (acceptors) would be viable if they are located within the Förster's distance.[47]

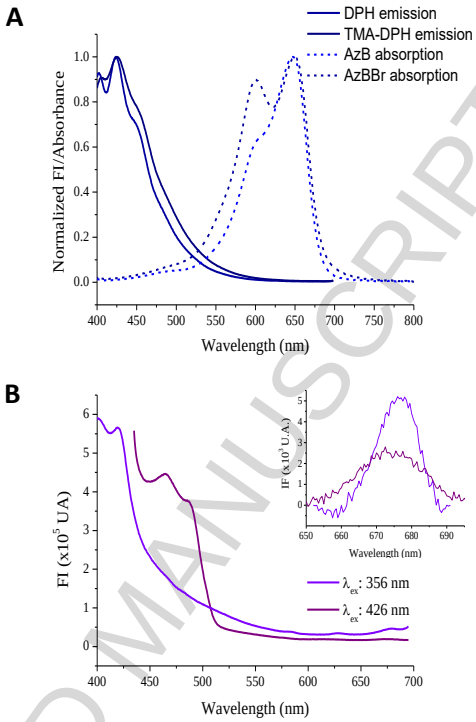

Figure 4: (**A**) Emission spectra of DPH and TMA-DPH (λ_{ex}= 356 nm) and absorption spectra of PSs. (**B**) Emission spectra of AzBBr excited at two different wavelengths. **Insert**: Emission spectra extended at around 675nm.

The emission spectra of the PSs were determined at λ_{ex}= 356 nm (the same λ used for exciting the probes) and at λ_{ex}= 426 nm (peak of $\lambda_{max\text{-}em}$ of the probes). AzBBr (**Figure 4B**) and AzB (not shown) exhibited a significant emission band between 400 nm and 500 nm and a lower intensity peak within a wavelength range of 650-700 nm (**insert, Figure 4B**). Because the former band overlapped with the emission region of DPH and TMA-DPH, it was not possible to analyze the decrease in the emission intensity of the donors during the energy transfer process. However, the increase in the emission intensity of the acceptors (PSs) in the presence of the donors at 679 nm would allow the assessment of the localization of the phenothiazine dyes in the liposomal membrane by the FRET experiments.

The variation of the FI of AzB and AzBBr encapsulated in the liposomes or free in solution as a function of the concentration of DPH and TMA-DPH is depicted in **Figure 5**. Note that in aqueous medium the emission of both PSs remained constant for all the concentrations of the probes evaluated. This behavior showed that the distance between the donor and acceptor molecules in PBS (without liposomes) did not allow the occurrence of FRET. In contrast, the samples incorporated in MLVs showed an exponential increase in the FI of AzB (**Figure 5A**) and AzBBr (**Figure 5B**), indicating that the FRET process was developed when the compounds were at an appropriate distance. This effect was considerably more intense for both dyes in the presence of TMA-DPH, indicating that the phenothiazine dyes were located mainly within the polar head region of the phospholipid bilayer of the evaluated liposomes.

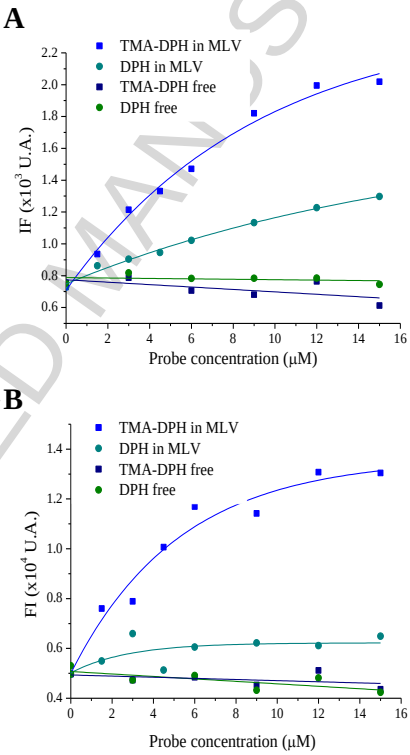

Figure 5: Effect of concentrations of probes on the FI of AzB (**A**) and AzBBr (**B**) free in solution and encapsulated in EPC-MLVs. λ_{ex}: 356 nm and $\lambda_{max\text{-}em}$: 679 nm.

In conclusion, AzB and AzBBr interacted with the membrane of EPC-MLVs and were preferably located on the hydrophilic surface of the lipid bilayer. These results are consistent with the amphiphilic character of the phenothiazine dyes whose molecular structures are depicted in **Figure S1** in the Supporting Information section.

3.5 Singlet oxygen quantum yields

As shown in **Table 1**, the phenothiazine dyes charged in EPC-MLVs increased the photochemical reactivity of both PSs, doubling the ϕ_Δ value of free AzBBr and increasing that of AzB by 60%. These results can be associated with the decrease in the aggregation of the phototherapeutic agents, mainly of the monobrominated derivative, as a consequence of the entrapment in the liposomal system (Section 3.2). It is important to remember that the incorporation of AzBBr in the selected vesicles partially reduced the formation of higher aggregates (**Figure 1**).

In addition, **Figure S4** shows that both irradiated MLVs without photodynamic agents and MLVs charged with any of the phenothiazine compounds in the dark did not produce ABDA degradation. These results corroborate that the photooxidation of ADBA was caused by the $^1O_2$ produced after the excitation of the PSs.

Table 1: Singlet oxygen quantum yields of free and encapsulated PSs.

PS	Abs_0	Slope ($x10^{-3}$)	ϕ_Δ
AzB*	0.16±0.02	1.25±0.03	1.0
AzB-MLV	0.09±0.01	1.14±0.06	1.6
AzBBr*	0.20±0.02	0.96±0.02	1.0
AzBBr-MLV	0.08±0.01	0.86±0.02	2.2

*Data obtained from ref.[29]

Consistent with the results obtained in this work, several authors have shown that the vehiculization of different PSs in liposomes, micelles and nanoparticles increases the ϕ_Δ of these compounds. This increase varies from 0.1 to 3.5, depending on the vehiculization system and the PS used.[20,29,48,49]

4 Conclusion

Multilamellar liposomes of EPC were selected for the development of third generation PSs because phenothiazine dyes exhibited a higher partitioning in EPC than in DPPC MLVs. This demonstrates that EPC is more efficient at preventing the formation of higher order aggregates. The structural

characteristics of AzB and AzBBr favor their location on the hydrophilic surface of the liposomal membrane. The phospholipid-PS ratio defined as optimal (15 mg / mL - 260 μM) allowed the encapsulation of $8x10^{-8}$ moles and $7x10^{-8}$ moles of AzB and AzBBr, respectively.

In addition, the vehiculization of these phototherapeutic agents in EPC-MLVs proved to be a successful strategy to improve the photochemical properties of the second generation PSs. In turn, the increase in the ϕ_Δ of the encapsulated AzB and AzBBr compared with free PSs can be explained by the decrease in the formation of higher aggregates. The $^1O_2$ production was enhanced between 60% and 100% as a consequence of the PS entrapment in EPC-MLVs. For these reasons, the liposomal systems developed in the present work are excellent alternatives to the evaluation of their efficacy in PDT and APDT. Further improvements should be made in the composition of these kinds of vectorization systems that tend to optimize the photochemical properties of the studied phenothiazine compounds. These strategies should be focused on favoring the lipid membrane partitioning of the PSs and/or on increasing the volume of the hydrophilic surface of the vectors.

Acknowledgements

This work was supported by grants from the Secretaría de Ciencia y Técnica (SeCyT) (Grants 366/16), the Consejo Nacional de Investigaciones Científicas y Tecnológicas (CONICET) (PIP 2014 11220130100650C GI), and the Agencia Nacional de Promoción Científica y Tecnológica (ANPCyT) (PICT-2012-2652). JV gratefully acknowledges the receipt of a fellowship from CONICET. JMS and MAP are career members of CONICET.

REFERENCES

[1] L.K. McKenzie, I. V. Sazanovich, E. Baggaley, M. Bonneau, V. Guerchais, J.A.G. Williams, J.A. Weinstein, H.E. Bryant, Metal Complexes for Two-Photon Photodynamic Therapy: A Cyclometallated Iridium Complex Induces Two-Photon Photosensitization of Cancer Cells under Near-IR Light, Chem. - A Eur. J. 23 (2017) 234–238. doi:10.1002/chem.201604792.

[2] L.M. Baltazar, A. Ray, D.A. Santos, P.S.P.S. Cisalpino, A.J. Friedman, J.D. Nosanchuk, Antimicrobial photodynamic therapy: An effective alternative approach to control fungal infections, Front. Microbiol. 6 (2015) 1–11. doi:10.3389/fmicb.2015.00202.

[3] Z. Hu, N. Oleinick, M.R. Hamblin, Photodynamic Therapy as an Emerging Treatment Modality for Cancer and Non-Cancer Diseases, J Anal Bioanal Tech. S1: e001 (2014). doi:10.4172/2155-9872.S1-e001.

[4] E.J. Hong, D.G. Choi, M.S. Shim, M. Suk, Targeted and effective photodynamic therapy for cancer using functionalized nanomaterials., Acta Pharm. Sin. B. 6 (2016) 297–307. doi:10.1016/j.apsb.2016.01.007.

[5] A.M. Lima, C.D. Pizzol, F.B.F. Monteiro, T.B. Creczynski-Pasa, G.P. Andrade, A.O. Ribeiro, J.R. Perussi, Hypericin encapsulated in solid lipid nanoparticles: Phototoxicity and photodynamic efficiency, J. Photochem. Photobiol. B Biol. 125 (2013) 146–154. doi:10.1016/j.jphotobiol.2013.05.010.

[6] G. Maria, F. Calixto, J. Bernegossi, L.M. De Freitas, C.R. Fontana, M. Chorilli, G.M. Calixto, J. Bernegossi, L.M. de Freitas, C.R. Fontana, M. Chorilli, Nanotechnology-Based Drug Delivery Systems for Photodynamic Therapy of Cancer: A Review., Molecules. 21 (2016) 342. doi:10.3390/molecules21030342.

[7] M. Dhayalan, M.I.J. Denison, M. Ayyar, N.N. Gandhi, K. Krishnan, B. Abdulhadi, Biogenic synthesis, characterization of gold and silver nanoparticles from Coleus forskohlii and their clinical importance, J. Photochem. Photobiol. B Biol. 183 (2018) 251–257. doi:10.1016/j.jphotobiol.2018.04.042.

[8] I. Herrmann, E. Supriyanto, S.K. Jaganathan, A. Manikandan, Advanced nanofibrous textile-based dressing material for treating chronic wounds, Bull. Mater. Sci. 41 (2018). doi:10.1007/s12034-017-1543-5.

[9] S.K. Jaganathan, M.P. Mani, A.F. Ismail, M. Ayyar, Manufacturing and characterization of novel electrospun composite comprising polyurethane and mustard oil scaffold with enhanced blood compatibility, Polymers (Basel). 9 (2017) 1–11. doi:10.3390/polym9050163.

[10] S.K. Jaganathan, M.P. Mani, M. Ayyar, E. Supriyanto, Engineered electrospun polyurethane and castor oil nanocomposite scaffolds for cardiovascular applications, J. Mater. Sci. 52 (2017) 10673–10685. doi:10.1007/s10853-017-1286-0.

[11] A.P. Subramanian, S.K. Jaganathan, A. Manikandan, K.N. Pandiaraj, N. Gomathi, E. Supriyanto, Recent trends in nano-based drug delivery systems for efficient delivery of phytochemicals in chemotherapy, RSC Adv. 6 (2016) 48294–48314. doi:10.1039/c6ra07802h.

[12] M.V. Vellayappan, S.K. Jaganathan, A. Manikandan, Nanomaterials as a game changer in the management and treatment of diabetic foot ulcers, RSC Adv. 6 (2016) 114859–114878. doi:10.1039/C6RA24590K.

[13] M. V. Vellayappan, J.R. Venugopal, S. Ramakrishna, S. Ray, A.F. Ismail, M. Mandal, A. Manikandan, S. Seal, S.K. Jaganathan, Electrospinning applications from diagnosis to treatment of diabetes, RSC Adv. 6 (2016) 83638–83655. doi:10.1039/c6ra15252j.

[14] K. Chitra, A. Manikandan, S. Arul Antony, Effect of Poloxamer on Zingiber Officinale Extracted Green Synthesis and Antibacterial Studies of Silver Nanoparticles, J. Nanosci. Nanotechnol. 16 (2016) 758–764. doi:10.1166/jnn.2016.10630.

[15] K. Chitra, A. Manikandan, S. Moortheswaran, K. Reena, S.A. Antony, Zingiber officinale extracted green synthesis of copper nanoparticles: Structural, morphological and antibacterial

studies, Adv. Sci. Eng. Med. 7 (2015) 710–716. doi:10.1166/asem.2015.1752.

[16] R. Lehner, X. Wang, S. Marsch, P. Hunziker, Intelligent nanomaterials for medicine: Carrier platforms and targeting strategies in the context of clinical application, Nanomedicine Nanotechnology, Biol. Med. 9 (2013) 742–757. doi:10.1016/j.nano.2013.01.012.

[17] C.K. Lim, J. Heo, S. Shin, K. Jeong, Y.H. Seo, W.D. Jang, C.R. Park, S.Y. Park, S. Kim, I.C. Kwon, Nanophotosensitizers toward advanced photodynamic therapy of Cancer, Cancer Lett. 334 (2013) 176–187. doi:10.1016/j.canlet.2012.09.012.

[18] E.S. Shibu, M. Hamada, N. Murase, V. Biju, Nanomaterials formulations for photothermal and photodynamic therapy of cancer, J. Photochem. Photobiol. C Photochem. Rev. 15 (2013) 53–72. doi:10.1016/j.jphotochemrev.2012.09.004.

[19] L.A. Muehlmann, G.A. Joanitti, J.R. Silva, J.P.F. Longo, R.B. Azevedo, Liposomal photosensitizers: Potential platforms for anticancer photodynamic therapy, Brazilian J. Med. Biol. Res. 44 (2011) 729–737. doi:10.1590/S0100-879X2011007500091.

[20] Y.T. Yang, C.T. Chen, T. Tsai, Absorption and fluorescence spectral properties of hematoporphyrin in liposomes, micelles, and nanoparticles, Dye. Pigment. 96 (2013) 763–769. doi:10.1016/j.dyepig.2012.09.014.

[21] N. Nombona, K. Maduray, E. Antunes, A. Karsten, T. Nyokong, Synthesis of phthalocyanine conjugates with gold nanoparticles and liposomes for photodynamic therapy, J. Photochem. Photobiol. B Biol. 107 (2012) 35–44. doi:10.1016/j.jphotobiol.2011.11.007.

[22] G.V. Roblero Bartolón, E. Ramón Gallegos, Uso de nanopartículas (NP) en la terapia fotodinámica (photodynamic therapy [PDT]) contra el cáncer, Gac. Med. Mex. 151 (2014) 85–98.

[23] P. Skupin-Mrugalska, J. Piskorz, T. Goslinski, J. Mielcarek, K. Konopka, N. Düzgünes, N. Düzgüneş, Current status of liposomal porphyrinoid photosensitizers, Drug Discov. Today. 18 (2013) 776–784. doi:10.1016/j.drudis.2013.04.003.

[24] M. Nisnevitch, F. Nakonechny, Y. Nitzan, Photodynamic antimicrobial chemotherapy by liposome-encapsulated water-soluble photosensitizers., Bioorg. Khim. 36 (2010) 396–402. doi:10.1134/S106816201003012X.

[25] M. Przybylo, D. Glogocka, J.W. Dobrucki, K. Fraczkowska, H. Podbielska, M. Kopaczynska, T. Borowik, M. Langner, The cellular internalization of liposome encapsulated protoporphyrin IX by HeLa cells, Eur. J. Pharm. Sci. 85 (2016) 39–46. doi:10.1016/j.ejps.2016.01.028.

[26] R.R. Deshmukh, S.V. Gawale, M.K. Bhagwat, A review on : Liposomes, World J. Pharm. Pharm. 5 (2016) 506–517.

[27] N.K. Verma, A. Roshan, Liposomes: A Targeted Drug Delivery System- A Review, Acta Medica Sci. 2 (2015) 65–70.

[28] J. Vara, C.S. Ortiz, Thiazine dyes: Evaluation of monomeric and aggregate forms, Spectrochim. Acta - Part A Mol. Biomol. Spectrosc. 166 (2016) 112–120. doi:10.1016/j.saa.2016.05.005.

[29] M.S. Gualdesi, C.I.A. Igarzabal, J. Vara, C.S. Ortiz, Synthesis and physicochemical properties of polyacrylamide nanoparticles as photosensitizer carriers, Int. J. Pharm. 512 (2016) 213–218. doi:10.1016/j.ijpharm.2016.08.051.

[30] M.N. Montes De Oca, J. Vara, L. Milla, V. Rivarola, C.S. Ortiz, Physicochemical properties and photodynamic activity of novel derivatives of triarylmethane and thiazine, Arch. Pharm. (Weinheim). 346 (2013) 255–265. doi:10.1002/ardp.201200437.

[31] S. Angeletti, J.M. Sanchez, L.W. Chamley, S. Genti-Raimondi, M.A. Perillo, StarD7 behaves as a fusogenic protein in model and cell membrane bilayers, Biochim. Biophys. Acta - Biomembr. 1818 (2012) 425–433. doi:10.1016/j.bbamem.2011.10.024.

[32] N.C. López Zeballos, J. Marino, M.C. García Vior, N. Chiarante, L.P. Roguin, J. Awruch, L.E. Dicelio, Photophysics and photobiology of novel liposomal formulations of 2,9(10), 16(17),23(24)-tetrakis[(2-dimethylamino)ethylsulfanyl]phthalocyaninatozinc(II), Dye. Pigment.

96 (2013) 626–635. doi:10.1016/j.dyepig.2012.11.005.

[33] M.A. Raviolo, J.M. Sanchez, M.C. Briñón, M.A. Perillo, Determination of liposome permeability of ionizable carbamates of zidovudine by steady state fluorescence spectroscopy, Colloids Surfaces B Biointerfaces. 61 (2008) 188–198. doi:10.1016/j.colsurfb.2007.08.004.

[34] A. Casas, C. Perotti, M. Saccoliti, P. Sacca, H. Fukuda, A.M. del C. Batlle, ALA and ALA hexyl ester in free and liposomal formulations for the photosensitisation of tumour organ cultures., Br. J. Cancer. 86 (2002) 837–842. doi:10.1038/sj.bjc.6600144.

[35] E. Lissi, M.L. Bianconi, A.T. do Amaral, E. de Paula, L.E.B. Blanch, S. Schreier, Methods for the determination of partition coefficients based on the effect of solutes upon membrane structure, BBA - Biomembr. 1021 (1990) 46–50. doi:10.1016/0005-2736(90)90382-X.

[36] J.M. Sánchez, A. del V. Turina, M.A. Perillo, Spectroscopic probing of ortho-nitrophenol localization in phospholipid bilayers, J. Photochem. Photobiol. B Biol. 89 (2007) 56–62. doi:10.1016/j.jphotobiol.2007.08.004.

[37] S.C. Hayden, L.A. Austin, R.D. Near, R. Ozturk, M.A. El-Sayed, Plasmonic enhancement of photodynamic cancer therapy, J. Photochem. Photobiol. A Chem. 269 (2013) 34–41. doi:10.1016/j.jphotochem.2013.06.004.

[38] O. Popovska, J. Simonovska, Z. Kavrakovski, V. Rafajlovska, An overview : methods for preparation and characterization of liposomes as drug delivery systems, Int. J. Pharm. Phytopharm. Res. 3 (2013) 182–189.

[39] A. Laouini, C. Jaafar-Maalej, I. Limayem-Blouza, S. Sfar, C. Charcosset, H. Fessi, Preparation, characterization and applications of liposomes: state of the art, J. Colloid Sci. Biotechnol. 1 (2012) 147–168. doi:10.1166/jcsb.2012.1020.

[40] M.G. Alvarez, M.N. Montes de Oca, M.E. Milanesio, C.S. Ortiz, E.N. Durantini, Photodynamic properties and photoinactivation of Candida albicans mediated by brominated derivatives of triarylmethane and phenothiazinium dyes., Photodiagnosis Photodyn. Ther. 11 (2014) 148–155. doi:10.1016/j.pdpdt.2014.03.005.

[41] S. Dhami, A.J. De Mello, G. Rumbles, S.M. Bishop, D. Phillips, A. Beeby, Phthalocyanine fluorescence at high concentration: dimers or reabsorption effect?, Photochem. Photobiol. 61 (1995) 341–346. doi:10.1111/j.1751-1097.1995.tb08619.x.

[42] D.M. Jameson, Introduction to Fluorescence, Taylor & Francis, Boca Raton, Florida, 2014.

[43] J. Sloniec-Myszk, U. Resch-Genger, A. Hennig, Chiral, J-Aggregate-Forming Dyes for Alternative Signal Modulation Mechanisms in Self-Immolative Enzyme-Activatable Optical Probes, J. Phys. Chem. B. 120 (2016) 877–885. doi:10.1021/acs.jpcb.5b10526.

[44] V. Martínez Martínez, F. López Arbeloa, J. Buñuelos Prieto, I. López Arbeloa, Characterization of Rhodamine 6G Aggregates Intercalated in Solid Thin Films of Laponite Clay. 2 Fluorescence Spectroscopy, J. Phys. Chem. B. 109 (2005) 7443–7450. doi:10.1021/jp047552e.

[45] M. Çamur, M. Durmuş, M. Bulut, Highly singlet oxygen generative water-soluble coumarin substituted zinc(II) phthalocyanine photosensitizers for photodynamic therapy, Polyhedron. 41 (2012) 92–103. doi:10.1016/j.poly.2012.04.034.

[46] L. Bene, T. Ungvári, R. Fedor, L. Damjanovich, Single-laser polarization FRET (polFRET) on the cell surface, Biochim. Biophys. Acta - Mol. Cell Res. 1843 (2014) 3047–3064. doi:10.1016/j.bbamcr.2014.07.011.

[47] R. Krishnaveni, P. Ramamurthy, Förster resonance energy transfer between acridinediones and selected fluorophores - Medium dependence, J. Lumin. 138 (2013) 242–250. doi:10.1016/j.jlumin.2013.01.025.

[48] B. Wang, J.-H. Wang, Q. Liu, H. Huang, M. Chen, K. Li, C. Li, X.-F. Yu, P.K. Chu, Rose-bengal-conjugated gold nanorods for in vivo photodynamic and photothermal oral cancer therapies., Biomaterials. 35 (2014) 1954–66. doi:10.1016/j.biomaterials.2013.11.066.

[49] K. Nawalany, A. Rusin, M. Kepczynski, P. Filipczak, M. Kumorek, B. Kozik, H. Weitman, B. Ehrenberg, Z. Krawczyk, M. Nowakowska, Novel nanostructural photosensitizers for photodynamic therapy: In vitro studies, Int. J. Pharm. 430 (2012) 129–140. doi:10.1016/j.ijpharm.2012.04.016.

Figure 1: Evaluation of aggregation of AzB and AzBBr, free and encapsulated in MLVs of EPC (**A** and **B**) or dpPC (**C** and **D**).

Figure 2: Fluorescence intensity (FI) vs. the concentration of AzB (**A**) and AzBBr (**B**) in PBS in the absence and in the presence of different DTs. **Insert**: Normalized fluorescence spectra at $\lambda_{max\text{-}em}$ at different concentrations of PSs. Arrows point to the direction observed with increasing concentration of PSs: (a) 1.5 μM; (h) 30 μM.

Figure 3: Encapsulation Efficiency (EE) of AzBBr in EPC MLVs as a function of lipid (**A**) and AzBBr (**B**) concentrations. **Insert**: Encapsulated mass of PS vs. the dye concentration used for the preparation of MLVs.

Figure 4: (**A**) Emission spectra of DPH and TMA-DPH (λ_{ex}= 356 nm) and absorption spectra of PSs. (**B**) Emission spectra of AzBBr excited at two different wavelengths. **Insert**: Emission spectra extended at around 675nm.

Figure 5: Effect of concentrations of probes on the FI of AzB (**A**) and AzBBr (**B**) free in solution and encapsulated in EPC-MLVs. λ_{ex}: 356 nm and $\lambda_{max\text{-}em}$: 679 nm.